

On the Free Radical Scavenging Capability of Carboxylated Single-Walled Carbon Nanotubes

Misaela Francisco-Marquez,[†] Annia Galano,^{*,†} and Ana Martínez[‡]

Departamento de Química, Universidad Autónoma Metropolitana-Iztapalapa, San Rafael Atlixco 186, Col. Vicentina, Iztapalapa, C. P. 09340, México D.F., Mexico, and Departamento de Materia Condensada y Criogenia, Instituto de Investigaciones en Materiales, Universidad Nacional Autónoma de México, Circuito Exterior S. N., Ciudad Universitaria, CP 04510, México D.F., Mexico

Received: January 4, 2010; Revised Manuscript Received: February 19, 2010

Density functional theory calculations have been used to model the efficiency of carboxylated single-walled carbon nanotubes (SWCNT) to act as free radical scavengers, relative to that of their corresponding nonfunctionalized partners. The exergonicity of the reactions between carboxylated SWCNTs and the studied free radicals was found to be dependent on the site of functionalization as well as on the site of reaction. The major conclusion from this work is that carboxylated SWCNTs are at least as good, or even better, free radical scavengers than their nonfunctionalized partners. It is proposed that the presence of $-\text{COOH}$ groups would increase the free radical scavenging activity of SWCNTs, provided that the coverage occurs in such an amount that there is enough free space on the walls for the reactions to take place. The reliability of the calculations reported in the present work has been tested by comparison with different levels of theory.

Introduction

Carbon nanotubes (CNTs) are cylindrical structures that can be thought of as a rolled-up graphene sheet. They have very unique properties, which make them ideal candidates for diverse nanotechnological applications. However, their lack of solubility limits the use of CNTs. Actually, pristine CNTs are insoluble in water and in all organic solvents.^{1–3} Chemical functionalization of CNTs is one of the possible ways to overcome this problem. The strategies for such a process can be categorized in three general groups:¹ (a) covalent attachment of chemical groups to the CNTs' walls, (b) noncovalent exohedral adsorption (wrapping) of various functional molecules, and (c) endohedral filling of the inner empty cavity.

Because, in the present work, we will be dealing with the CNTs' structure modified by covalent attachments to the tubes' walls, we will focus only on strategy (a). Oxidation of CNTs is one example of such a strategy. It has been reported that the surface of oxidized nanotubes is covered by carboxylic ($-\text{COOH}$), carbonyl ($-\text{C}=\text{O}$), and hydroxyl ($-\text{COH}$) groups, in the approximate proportions of 4:2:1.⁴ Consequently, the oxidized nanotubes disperse better in solution than the raw material. In addition, it has been proposed that the most important advantage of oxidation is that the presence of the above-mentioned groups should increase the chemical reactivity and specificity of the otherwise rather inert carbon surface.⁵ Another important observation is that the surface reactions are not limited to the carboxylic groups.⁵

Carboxylation is definitively an important structural modification of CNTs. It should be noticed that CNT production always yields contaminated samples.⁶ The most frequent contaminants are other types of carbon particles, amorphous material, and metals.⁶ For single-walled carbon nanotubes (SWCNTs), puri-

fications by reflux in nitric acid⁷ as well as by partial oxidation in $\text{H}_2\text{SO}_4/\text{HNO}_3$ solutions⁸ have been developed. As a consequence of such processes, carboxylic and other hydrophilic groups are present on the purified SWCNTs.^{7,9} Refluxing in nitric acid has also been proposed by Ebbesen et al.¹⁰ and Liu et al.¹¹ for wetting SWCNTs, also leading to carboxylation of the tubes.^{11–13}

Regarding biomedical applications, a major concern about carbon nanotubes is their possible toxicity. In addition to their increased solubility, another important feature of carboxylated SWCNTs is that it has been demonstrated that they have lower toxicity than the nonfunctionalized tubes.¹⁴ Therefore, for the intended purpose investigated in this work, carboxylated SWCNTs are a promising choice and the main idea is to use them as free radical traps.

It has been recently proposed that CNTs and, in particular, SWCNTs are very efficient as free radical scavengers.^{15–20} This valuable property could have useful biomedical and environmental applications, where free radicals are known to be very damaging species. However, this is still an emergent area of research, and consequently, there are several open related questions.²⁰ So far, the free radical scavenging activity of CNTs has not been tested for functionalized tubes. Therefore, it is the main aim of the present work to investigate the relationship between the free radical scavenging activity and the presence of carboxyl groups on the SWCNTs' walls.

Finite fragments of (3,3) armchair and (5,0) zigzag SWCNTs, with two $-\text{COOH}$ groups at their ends or at central sites, and four different free radicals ($\bullet\text{OH}$, $\bullet\text{OOH}$, $\bullet\text{OCH}_3$, and $\bullet\text{CH}_3$) have been used for that purpose. Different sites of reactions have been modeled using density functional theory (DFT).

Computational Details

Electronic structure calculations have been performed with the Gaussian 03²¹ package of programs. Full geometry optimizations and frequency calculations were carried out for all the stationary points using the B3LYP hybrid HF density functional

* To whom correspondence should be addressed. E-mail: agalano@prodigy.net.mx.

[†] Universidad Autónoma Metropolitana-Iztapalapa.

[‡] Universidad Nacional Autónoma de México.

and the 3-21G basis set. No symmetry constraints have been imposed in the geometry optimizations. The energies of all the stationary points were improved by single-point calculations at the B3LYP/6-311+G(d) level of theory. Thermodynamic corrections at 298 K were included in the calculation of relative energies. Spin-restricted calculations were used for closed shell systems and unrestricted ones for open shell systems. Local minima were identified by the number of imaginary frequencies (NIMAG = 0). It seems worthwhile to emphasize the fact that any theoretical model aiming to make predictions concerning practical applications must be analyzed in terms of Gibbs free energies, which implies the necessity of performing frequency calculations that are particularly expensive. Accordingly, it seems a better compromise to perform frequency calculations at a low level of theory than increase the level and analyze the results only in terms of electronic energy. In addition and as will be reported below, the frequency calculations performed for the studied systems at the B3LYP/3-21G level of theory are in good agreement with experimental results.

The stationary points were first modeled in the gas phase (vacuum), and solvent effects were included a posteriori by single-point calculations using a polarizable continuum model, specifically, the integral-equation formalism (IEF-PCM)^{22–25} at the B3LYP/6-311+G(d) level of theory, with benzene and water as solvents for mimicking nonpolar and polar environments, respectively. The solvent cage effects have been included in the calculations of the Gibbs free energies of reaction according to the corrections proposed by Okuno,²⁶ taking into account the free volume theory.²⁷ These corrections are in good agreement with those independently obtained by Ardura et al.²⁸ and have been successfully used by other authors.^{29–34} This correction is important because the packing effects of the solvent reduce the entropy loss associated with any addition reaction.

Discussion and Results

Geometries. The first addition reactions of four different free radicals ($\bullet\text{OH}$, $\bullet\text{OOH}$, $\bullet\text{OCH}_3$, and $\bullet\text{CH}_3$) with nonfunctionalized and double COOH functionalized finite fragments of (3,3) armchair and (5,0) zigzag SWCNTs, about 11 Å long, have been studied. Two different sites of functionalization have been taken into account, with the two $-\text{COOH}$ groups at the ends of the tubes or at central sites (Figure 1). Only one configuration for the relative position of the functionalization groups has been considered in the present work, that with the two carboxylic groups opposite to each other. It should be noticed that there are many other configurations that are also possible, like with the two groups next to each other, for example, and the influence of their relative location on the SWCNT reactions with free radicals might deserve further studies. However, such influence is expected to be proportional to that described in the present study. The dangling bonds at the ends of the SWCNTs have been saturated by hydrogen atoms to avoid unwanted distortions. The reactions have been computed in the gas phase as well as in water and benzene solution, aiming for environmental and biological applications.

For pristine and terminally carboxylated SWCNTs, only one addition site has been considered: at the central hexagon. It has been chosen to avoid unwanted interactions with the terminal H atoms. For SWCNTs functionalized at the center of the fragment, four different sites of reaction have been taken into account, namely, (1) at the C atom next to that where the $-\text{COOH}$ group is attached to, that is, one C–C bond apart; (2) two C–C bonds apart from the closest functionalization site; (3) three C–C bonds apart from both functionalization sites, in

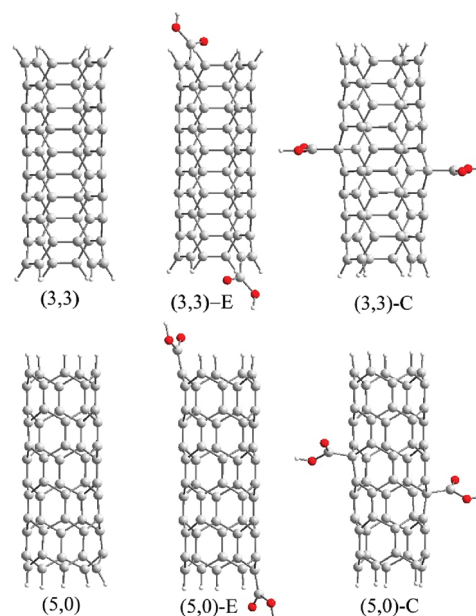


Figure 1. Studied SWCNT fragments and acronyms used in this work.

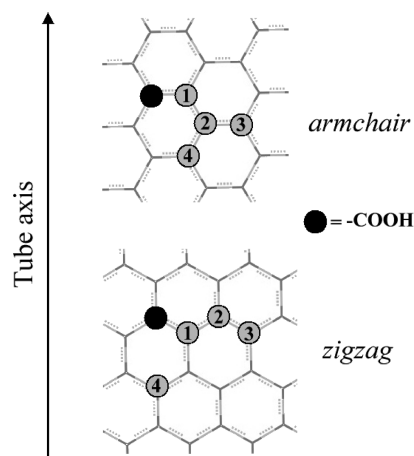


Figure 2. Schematic representation of the different sites of reaction.

the direction perpendicular to the tube axis; and (4) at the para site with respect to the closest carboxyl group. All the studied reaction sites are schematically represented in Figure 2, and the products of the reactions with the OH radical are shown as an example in Figure 3.

The most relevant geometrical parameter related to the studied reactions is the distance of the newly formed bond. The values of such distances for all the fully optimized products of reaction are reported in Table 1. The influence of the site of reaction on these distances was found to be negligible. The $d(\text{C}-\text{O})$ distances for the $\bullet\text{OH}$ and $\bullet\text{OCH}_3$ addition products range from 1.45 to 1.48 Å in all the studied cases. The $d(\text{C}-\text{C})$ distances corresponding to $\bullet\text{CH}_3$ addition products vary from 1.55 to 1.58 Å and the $d(\text{C}-\text{O})$ distance in the $\bullet\text{OOH}$ adducts from 1.48 to 1.49 Å. Among all the newly formed C–O bonds, those corresponding to the $\bullet\text{OOH}$ adducts systematically show the largest bond distance. Other relevant geometrical features are those corresponding to changes in the bond distance of the radical fragments attached to the tubes, compared to their values in the free radicals. The $d(\text{O}-\text{H})$ and $d(\text{C}-\text{H})$ in the hydroxyl and methyl moieties do not show any significant variation after the addition processes take place, and therefore, they are not

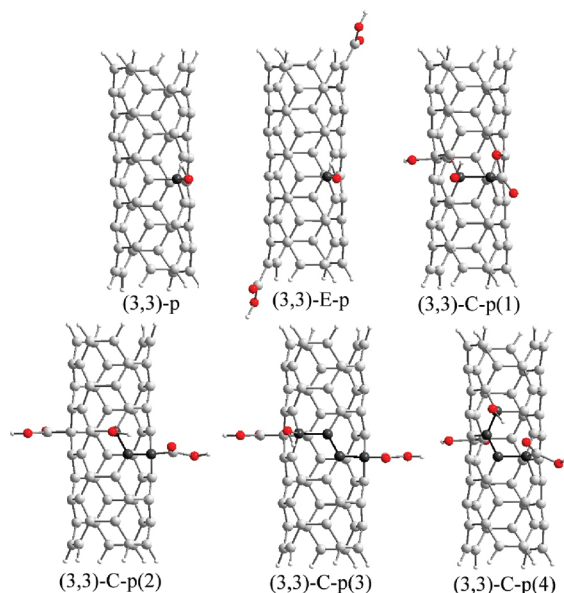


Figure 3. Studied products of the reactions of the OH radical with the nonfunctionalized and COOH-functionalized (3,3) SWCNT fragments.

TABLE 1: Selected Geometrical Parameters (Å) of the Addition Products

radical distance	•OH		•CH ₃		•OOH		•OCH ₃	
	<i>d</i> (C–O)	<i>d</i> (C–C)	<i>d</i> (C–O)	<i>d</i> (O–O)	<i>d</i> (C–O)	<i>d</i> (O–C)	<i>d</i> (C–O)	<i>d</i> (O–C)
(3,3)-p	1.46	1.55	1.49				1.46	
(3,3)-E-p	1.46	1.55	1.49	1.52	1.46	1.46		
(3,3)-C-p(1)	1.47	1.56	1.48	1.52	1.47	1.47		
(3,3)-C-p(2)	1.46	1.56	1.48	1.52	1.48	1.47		
(3,3)-C-p(3)	1.45	1.55	1.48	1.52	1.46	1.47		
(3,3)-C-p(4)	1.43	1.55	1.48	1.52	1.45	1.46		
(5,0)-p	1.46	1.56	1.48			1.46		
(5,0)-E-p	1.47	1.56	1.48	1.52	1.47	1.47		
(5,0)-C-p(1)	1.45	1.55	1.48	1.52	1.46	1.48		
(5,0)-C-p(2)	1.46	1.56	1.48	1.52	1.46	1.47		
(5,0)-C-p(3)	1.46	1.56	1.48	1.52	1.46	1.47		
(5,0)-C-p(4)	1.47	1.58	1.48	1.52	1.47	1.48		

reported in Table 1. The *d*(O–O) distance in the peroxy moiety and the *d*(O–C) distance in the alkoxy group, on the other hand, are significantly enlarged in the adducts, with respect to their values in the free radicals. The *d*(O–O) distance in the free •OOH radical is 1.42 Å, at the level of theory used, whereas in the addition products, it was found to be systematically 0.1 Å longer for all the modeled systems. The *d*(O–C) distance was found to be 1.43 Å in the free •OCH₃ radical, whereas it ranges from 1.46 to 1.48 Å in the alkoxy fragment of the addition products.

IR Spectra. The infrared (IR) spectra of the functionalized tubes as well as of the products of reaction have been also analyzed. The O–H and C=O stretching bands corresponding to carboxylic groups have been used to experimentally identify carboxylated nanotubes. The values of their calculated frequencies, compared to the average values from experimental determinations, are shown in Table 2. Because our frequency calculations have been performed at a modest level of theory, due to the large size of the studied systems, this comparison helps to assess the reliability of the thermodynamic corrections used in the present work. As the values in Table 2 show, the correspondence between experimental and nonscaled calculated values is good. The average errors of the calculated values are

TABLE 2: Frequencies (cm⁻¹) of the O–H and C=O Stretching Bands Corresponding to the Carboxylic Groups in Functionalized SWCNTs

	$\nu_{\text{O-H}}$	$\nu_{\text{C=O}}$
(3,3)-E	3499	1745
(3,3)-C	3478	1799
(5,0)-E	3495	1685
(5,0)-C	3481	1790
experimental ^a	3435	1710

^a Average from refs 35–38.

TABLE 3: Frequencies (cm⁻¹) of the O–H and C=O Stretching Bands Corresponding to the Carboxylic Groups in the Addition Products

	(3,3)		(5,0)	
	$\nu_{\text{O-H}}$	$\nu_{\text{C=O}}$	$\nu_{\text{O-H}}$	$\nu_{\text{C=O}}$
E–OH	3501	1744	3493	1674
E–OOH	3501	1744	3493	1677
E–OCH ₃	3501	1744	3492	1673
E–CH ₃	3501	1743	3493	1687
C–OH(1)	3477	1801, 1797	3480, 3475	1820, 1795
C–OH(2)	3478, 3471	1796, 1757	3480, 3469	1792, 1778
C–OH(3)	3477	1795	3483	1790
C–OH(4)	3478, 3465	1796, 1732	3481, 3462	1797, 1793
C–OOH(1)	3486, 3477	1798, 1773	3479, 3470	1795, 1722
C–OOH(2)	3478, 3472	1796, 1744	3481, 3472	1792, 1779
C–OOH(3)	3478	1798	3481	1792
C–OOH(4)	3477, 3474	1798, 1743	3498, 3481	1794, 1792
C–OCH ₃ (1)	3483, 3477	1798, 1785	3481, 3480	1790, 1768
C–OCH ₃ (2)	3468, 3466	1793, 1772	3481, 3468	1792, 1778
C–OCH ₃ (3)	3478	1795	3483	1792
C–OCH ₃ (4)	3477	1796	3481, 3475	1797, 1793
C–CH ₃ (1)	3477, 3471	1796, 1765	3481, 3470	1790, 1780
C–CH ₃ (2)	3477, 3474	1796, 1775	3481, 3474	1791, 1787
C–CH ₃ (3)	3478	1796	3482	1795
C–CH ₃ (4)	3478, 3476	1797, 1773	3481, 3470	1793, 1781

lower than 2% and 3% for O–H and C=O stretchings, respectively.

The frequency values corresponding to these two bands after the free radicals are attached to the functionalized SWCNTs structures are reported in Table 3. As these values show, the shifting in the bands' positions is negligible. The most significant effect arises for those products where the attached moiety is close to the –COOH groups. In such cases, the bands corresponding to $\nu_{\text{O-H}}$ and $\nu_{\text{C=O}}$ vibrations split into two, indicating the interaction between the neighbor functional groups. The difference in frequencies between the twin bands ranges from about 5 to 20 cm⁻¹.

In addition to the bands characteristic of carboxylic groups, some other bands representative of the newly attached groups, after the addition reactions, have also been identified, and their frequency values are provided in the Supporting Information, in Tables 2S and 3S. For the OH adducts, the vibrations corresponding to the O–H stretching in this moiety appear within the range of 3250–3470 cm⁻¹, whereas the equivalent vibrations for the OOH adducts were found from 3200 to 3390 cm⁻¹. The O–O stretching of the peroxy group was found in the range of 950–980 cm⁻¹. For the adducts arising as products of the reactions between SWCNTs and the OCH₃ and CH₃ free radicals, the asymmetric ($\nu_{\text{C-H}}^{\text{(A)}}$) and symmetric ($\nu_{\text{C-H}}^{\text{(S)}}$) stretchings of the CH₃ moieties were found in the 3080–3190 and 3010–3070 cm⁻¹ regions, respectively. The umbrella (rocking) modes of the methyl groups (δ_{CH_3}) arise within the range of 1440–1490 cm⁻¹. They are in good agreement with the values reported by Saini et al.³⁹

TABLE 4: Entropy Terms ($T\Delta S$, in kcal/mol) Involved in the Studied Addition Reactions at 298.15 K

	•OH	•OCH ₃	•OOH	•CH ₃
		gas		
n33-p	-10.24	-12.20	-11.84	-11.75
n33E-p	-10.34	-12.44	-12.23	-11.91
n33C-p(1)	-11.41	-13.32	-12.45	-12.52
n33C-p(2)	-10.43	-12.02	-13.04	-11.63
n33C-p(3)	-10.25	-12.31	-12.00	-11.68
n33C-p(4)	-11.01	-11.76	-12.74	-12.00
n50-p	-10.30	-11.99	-11.67	-11.53
n50E-p	-10.59	-12.70	-12.07	-11.69
n50C-p(1)	-12.08	-13.83	-14.34	-13.20
n50C-p(2)	-9.99	-11.87	-11.79	-11.82
n50C-p(3)	-10.17	-12.05	-12.00	-12.10
n50C-p(4)	-10.94	-13.33	-12.45	-12.56
		solution ^a		
n33-p	-5.81	-7.77	-7.41	-7.32
n33E-p	-5.91	-8.01	-7.80	-7.48
n33C-p(1)	-6.98	-8.89	-8.02	-8.09
n33C-p(2)	-6.00	-7.59	-8.61	-7.20
n33C-p(3)	-5.82	-7.88	-7.57	-7.25
n33C-p(4)	-6.58	-7.33	-8.31	-7.57
n50-p	-5.87	-7.56	-7.24	-7.10
n50E-p	-6.16	-8.27	-7.64	-7.26
n50C-p(1)	-7.65	-9.40	-9.91	-8.77
n50C-p(2)	-5.56	-7.44	-7.36	-7.39
n50C-p(3)	-5.74	-7.62	-7.57	-7.67
n50C-p(4)	-6.51	-8.90	-8.02	-8.13

^a The entropy evolution for the reactions studied in benzene and water solutions are identical in the present case because frequency calculations were performed only in the gas phase, where geometry optimizations were carried out.

Energies. Enthalpies (ΔH), entropies ($T\Delta S$), and Gibbs (ΔG) free energies of reaction, computed at 298.15 K, for all the studied addition processes are reported in Table 5. The energies of reaction, including zero-point energy corrections, are provided in Table 1S in the Supporting Information. All the modeled addition reactions were found to be exothermic, and most of them were found to be exergonic. The most exothermic and most exergonic processes were found to be those corresponding to the reactions with the OH radical, which is a logical finding due to the known high reactivity of this radical.

From this point forward, we will focus our discussion on the Gibbs free energies of reaction. It seems worthy to emphasize the importance of considering Gibbs free energies when analyzing the viability of chemical processes. This is particularly important for addition reactions, which is the case of the present study, because they necessarily involve a significant entropy loss. To illustrate the relevance of the entropy to the studied reactions, the corresponding $T\Delta S$ values are reported in Table 4. It should be noticed that, for reactions in solution, it is also important to consider the solvent cage effects. If they are not taken into account and the translational degrees of freedom in solution are treated as in the gas phase, the cost associated with their loss when two or more molecules form a complex system in solution is overestimated, and consequently, these processes are overpenalized in solution. As the values in Table 4 show, the entropy changes involved in the studied addition reactions are relative large and they must be taken into account. Logically, based on the explanation above, the entropy loss is systematically larger in the gas phase, ranging from ~ 10 to ~ 14 kcal/mol, than in solution (~ 5 to ~ 10 kcal/mol). In general, from all the modeled additions, the smallest entropy loss corresponds to the formation of •OH products (2) and (3), when this radical is attached to the (5,0) carboxylated fragment. The largest

entropy loss was found for the formation of product (1), corresponding to the •OOH reaction with the (5,0) carboxylated fragment.

As stated in the Introduction, the main goal of the present work is to investigate if the presence of carboxyl groups in the structure of SWCNTs affects their ability to scavenge free radicals. According to the values reported in Table 5, the first thing that highlights is that the answer to that question is yes; the presence of -COOH groups definitively affects the free radical scavenging activity of SWCNTs. One exception was found, however, for the (3,3) fragment functionalized at the open ends of the tube ((3,3)-E). In this case and regardless of the polarity of the modeled environment, the free radical scavenging activity is almost the same than that of the nonfunctionalized fragment. This result seems to be a logical finding because the site of reaction is far enough from the carboxylic groups. For the (5,0)-E structure, despite the fact that carboxylated sites are equally far from the reaction site, the exergonicity of the addition reactions was found to be significantly decreased with respect to (5,0) for all the modeled radicals and in all the modeled environments. Therefore, at least for ultrashort SWCNTs, as those studied in the present work, carboxylations at the end of zigzag tubes apparently decrease their free radical scavenging activity. It is important to notice, however, that even the exergonicity is decreased; terminally carboxylated zigzag SWCNTs are still expected to be great free radical scavengers, with their ΔG of reaction ranging from -11 to -40 kcal/mol, depending on the reacting radical and on the polarity of the environment.

The following logical question is if the presence of the carboxyl groups in the walls of the SWCNTs increases or decreases such activity. In this case, the viability of the radical addition processes was found to depend on the reaction site as well as on the SWCNTs helicity. The exergonicity of the reactions involving the centrally carboxylated armchair fragment ((3,3)-C) was found to increase, with respect to that of the pristine tube, for reaction sites (1), (3), and (4). In general, the increase in exergonicity was found to be less significant for reactions taking place at site (4) than for those at sites (1) and (3). Radical additions to site (2), on the other hand, were found to be systematically less exergonic than the processes involving the corresponding nonfunctionalized SWCNT. This was found to be the case, regardless of the polarity of the environment and for all the studied free radicals.

For the studied zigzag fragment ((5,0)-C), reactions at site (1) were found to be more exergonic than those involving its nonfunctionalized partner (Table 5). The largest difference was found for the reactions involving the •OH radical and the smallest difference for the •CH₃ radical. In general, the difference on exergonicity, with respect to the pristine tube, was found to be smaller for polar environments. The exergonicity of the reactions at all the other studied sites of reaction was found to be lower than that of the pristine (5,0) fragment. However, in all the cases, the studied processes are exergonic, with ΔG values large enough to overcome any inaccuracy of the employed methodology. This suggests that zigzag carboxylated nanotubes should be good free radical scavengers. The above-described relative scavenging power was found to be the same for all the studied free radicals and in all the studied environments. Therefore, it can be concluded that, for carboxylated zigzag SWCNTs, at least for short tubes, the ortho site with respect to the -COOH group becomes the preferred site of reaction. It should be noticed, however, that all the studied

TABLE 5: Enthalpies (ΔH) and Gibbs (ΔG) Free Energies of Reaction, in kcal/mol, Computed at 298 K

	•OH		•CH ₃		•OOH		•OCH ₃	
	ΔH	ΔG	ΔH	ΔG	ΔH	ΔG	ΔH	ΔG
				gas				
(3,3)-p	-43.7	-33.4	-36.4	-24.7	-17.8	-5.9	-28.1	-15.9
(3,3)-E-p	-42.8	-32.4	-35.9	-24.0	-17.1	-4.9	-27.7	-15.2
(3,3)-C-p(1)	-57.3	-45.9	-49.0	-36.5	-31.8	-19.4	-39.6	-26.3
(3,3)-C-p(2)	-30.9	-20.4	-20.9	-9.3	-6.9	6.1	-14.1	-2.1
(3,3)-C-p(3)	-54.9	-44.6	-48.4	-36.8	-27.7	-15.7	-39.3	-27.0
(3,3)-C-p(4)	-49.1	-38.1	-38.3	-26.3	-29.2	-16.4	-31.9	-20.1
(5,0)-p	-54.6	-44.3	-46.9	-35.4	-29.1	-17.4	-39.7	-27.7
(5,0)-E-p	-48.8	-38.2	-41.3	-29.7	-23.2	-11.2	-32.6	-19.9
(5,0)-C-p(1)	-69.3	-57.5	-55.1	-41.9	-43.2	-28.8	-49.8	-36.0
(5,0)-C-p(2)	-46.9	-36.9	-35.8	-23.9	-20.0	-8.2	-32.2	-20.3
(5,0)-C-p(3)	-46.4	-36.2	-42.7	-30.6	-22.5	-10.5	-32.2	-20.1
(5,0)-C-p(4)	-43.5	-32.6	-31.7	-19.1	-18.9	-6.5	-29.3	-15.9
				benzene				
(3,3)-p	-42.4	-36.6	-36.3	-29.0	-16.7	-9.3	-27.6	-19.8
(3,3)-E-p	-41.3	-35.4	-35.7	-28.2	-16.0	-8.2	-27.0	-19.0
(3,3)-C-p(1)	-54.1	-47.1	-48.0	-40.0	-29.4	-21.3	-37.9	-29.0
(3,3)-C-p(2)	-28.4	-22.4	-20.2	-13.0	-4.3	4.3	-13.1	-5.5
(3,3)-C-p(3)	-53.2	-47.4	-47.8	-40.6	-25.9	-18.3	-38.0	-30.1
(3,3)-C-p(4)	-45.9	-39.4	-37.5	-30.0	-25.7	-17.4	-30.6	-23.2
(5,0)-p	-53.3	-47.4	-46.3	-39.2	-27.9	-20.6	-38.7	-31.2
(5,0)-E-p	-47.0	-40.9	-40.8	-33.6	-21.5	-13.9	-31.4	-23.1
(5,0)-C-p(1)	-71.3	-63.6	-53.4	-44.6	-39.2	-29.3	-47.4	-38.0
(5,0)-C-p(2)	-45.0	-39.4	-34.2	-26.8	-18.1	-10.7	-30.4	-22.9
(5,0)-C-p(3)	-44.0	-38.3	-41.0	-33.3	-20.1	-12.5	-30.5	-22.9
(5,0)-C-p(4)	-39.8	-33.3	-29.9	-21.8	-15.8	-7.7	-26.8	-17.9
				water				
(3,3)-p	-41.8	-36.0	-36.3	-29.0	-16.0	-8.6	-27.1	-19.4
(3,3)-E-p	-40.6	-34.7	-35.6	-28.1	-15.2	-7.3	-26.5	-18.5
(3,3)-C-p(1)	-50.1	-43.1	-46.5	-38.4	-26.5	-18.5	-35.5	-26.6
(3,3)-C-p(2)	-24.9	-18.9	-18.9	-11.7	-0.6	8.0	-12.3	-4.7
(3,3)-C-p(3)	-51.3	-45.5	-46.8	-39.5	-24.2	-16.6	-36.3	-28.4
(3,3)-C-p(4)	-41.3	-34.7	-36.4	-28.8	-19.8	-11.5	-28.8	-21.4
(5,0)-p	-52.0	-46.1	-45.4	-38.3	-26.8	-19.5	-37.8	-30.3
(5,0)-E-p	-45.1	-39.0	-40.1	-32.8	-19.6	-12.0	-29.8	-21.6
(5,0)-C-p(1)	-61.9	-54.2	-50.1	-41.3	-33.2	-23.3	-43.4	-34.0
(5,0)-C-p(2)	-42.0	-36.5	-31.0	-23.6	-15.7	-8.3	-27.7	-20.2
(5,0)-C-p(3)	-40.0	-34.3	-37.0	-29.4	-16.0	-8.4	-28.3	-20.7
(5,0)-C-p(4)	-34.2	-27.7	-26.4	-18.3	-11.1	-3.1	-23.0	-14.1

free radicals are small-sized and this behavior can change for large-sized free radicals due to steric hindrance.

Analyzing all the above-discussed results together, the major conclusion from this work is that carboxylated SWCNTs are at least as good, or even better, free radical scavengers than their nonfunctionalized partners. In fact, assuming that reactions take place at the most reactive sites, it can be concluded that the presence of $-\text{COOH}$ groups would increase the free radical scavenging activity of SWCNTs, provided that the coverage occurs in such an amount that there is enough free space on the walls for the reactions to take place. All these reactivity-related findings are in line with the predictions by Ebbesen et al.⁵ that the reactivity of the nanotubes should be increased when carboxylated and that the surface reactions are not limited to the carboxylic groups.

Reliability of the Methodology Used. Because there are no experimental data to compare with, the reliability of the calculations reported in the present work has been tested by comparison with other levels of theory. The reactions of the OH radical with coronene and the nonfunctionalized SWCNTs have been used to that purpose. They have been modeled only in the gas phase and in benzene solutions because neither coronene nor pristine SWCNTs are soluble in water. Coronene has been chosen for this test because it is the smallest polycyclic

aromatic hydrocarbon having the essential structural elements of graphene. Therefore, theoretical models of graphite, soot, or carbon nanotube walls often employ coronene as a model for representing a finite section of a carbon surface.⁴⁰⁻⁴² In addition, its size allows testing a larger variety of levels of theory at a reasonable computational cost.

The results obtained with the B3LYP/6-311+G(d)//3-21G level of theory (the one used in this work) have been compared with the results obtained by other functionals and the same basis sets as well as with results obtained with the B3LYP functional and a larger basis set for geometry optimizations and frequency calculations (B3LYP/6-311+G(d)//6-31+g(d)). The other functionals used are M06-2X,⁴³ TPSS,⁴⁴ BMK,⁴⁵ BHandHLYP,⁴⁶ and the newly developed empirical dispersion corrected variations⁴⁷ of B2PLYP.⁴⁸

The most relevant geometrical parameter for the OH radical reactions with coronene and SWCNTs is the C–O distance in the formed OH radical adducts. Only slight differences arise for it when geometries are optimized at different levels of theory (Table 6). The effect of increasing the basis set in the geometry optimization process is a shortening of $d(\text{C}-\text{O})$ by 0.02 Å for coronene and the pristine (5,0) SWCNT and by 0.03 Å for the (3,3) tube. The $d(\text{C}-\text{O})$ value obtained at the B3LYP/6-311+G(d)//3-21G level of theory is in the middle of the range

TABLE 6: Distance of the C–O Bond Formed in the Radical Adduct, Obtained by Full Geometry Optimizations at Different Levels of Calculation

	coronene	(3,3) SWCNT	(5,0) SWCNT
B3LYP/6-311+G(d)//3-21G	1.51	1.46	1.46
B3LYP/6-311+G(d)//6-31+g(d)	1.49	1.43	1.44
M062x/6-311+G(d)//3-21G	1.49	1.44	
TPSS/6-311+G(d)//3-21G	1.53	1.47	
BMK/6-311+G(d)//3-21G	1.49		
BHandHLYP/6-311+G(d)//3-21G	1.48		
B2PLYPD/6-311+G(d)//3-21G	1.50		

predicted by the different tested functionals, 1.48–1.53 Å. The largest functional-dependent variation was found between the BHandHLYP and the TPSS, which leads to the extreme values of the range, respectively. Therefore, it can be concluded that all the tested levels of calculation produce equivalent geometries.

The energetic of the studied reactions is the main aspect of the present study because the predictions of the viability of the intended processes are based on the energy changes associated with them. Accordingly, it seems worthwhile to analyze the effects of the level of theory used on our energetic predictions. All the tested levels of theory predict the reactions of •OH with SWCNTs to be significantly exergonic (Table 8), which means that our conclusions regarding the viability of the studied reactions are reliable. For the (3,3) SWCNTs, the calculated ΔG values range from –33.42 to –37.17 kcal/mol and from –42.41 to –47.64 kcal/mol for the gas phase and benzene solutions, respectively. In both media, the least negative value corresponds just to the B3LYP/6-311+G(d)//3-21G level of theory, which means that using a more sophisticated functional, such as M06-2X, leads to even larger exergonicities. In addition, the •OH reaction with coronene is predicted to be endergonic by all the tested levels of theory. In this case, the ΔG value

obtained at the B3LYP/6-311+G(d)//3-21G level of theory lies in between those obtained with the other levels of theory. In general, it can be stated that the trends on the viability of the studied chemical reactions (exergonic or endergonic) is similarly predicted by all the levels of theory used. The energies of reaction were found to be more sensitive to the chosen functional than to the size of the basis sets, and therefore, both effects will be discussed next in detail and separately.

As it is evident from the values reported in Tables 7 and 8, the effect of increasing the basis set, from 3-21G to 6-31G(d) for the tubes and to 6-31+G(d) for coronene, is only minor. In the particular case of the SWCNTs, which are the target molecules in this work, the effect of increasing the basis set on the ΔE , ΔH , and ΔG of reaction is actually negligible (less than or about 0.5 kcal/mol), whereas the increase on the computing time is quite significant, in particular, for frequency calculations. For the reaction •OH + coronene, the largest effects arising from increasing the basis set were found for the ΔG of reaction in the gas phase (+1.17 kcal/mol) and for the ΔH in benzene solution (–1.23 kcal/mol). In both cases, the changes are around the generally accepted computational accuracy (1 kcal/mol), not intended in the present work because it is rarely achieved for chemical systems as large-sized as those studied here. It is interesting to notice that such a small influence of the basis set size rules out a relevant role of the basis set superposition error on the studied addition reactions. Similar outcomes have been recently reported and justified by the cancellation of different errors arising from basis set truncation.⁴⁹

Even though the general trends do not seem to be functional-dependent, the effect of the functional of choice on the energetic of the studied reactions is not negligible. For the coronene + •OH reaction, the ΔG values calculated with the BHandHLYP and B2PLYPD functionals are higher (more positive) than those obtained with the B3LYP functional. On the other hand, ΔG values calculated with the M06-

TABLE 7: Energies^a (ΔE), Enthalpies (ΔH), and Gibbs (ΔG) Free Energies of the Coronene + •OH Reaction, in kcal/mol, Computed at 298 K, Using Different Levels of Theory

	gas		benzene			
	ΔE	ΔH	ΔG	ΔE	ΔH	ΔG
B3LYP/6-311+G(d)//3-21G	–0.48	–1.41	8.78	0.91	–0.02	10.18
B3LYP/6-311+G(d)//6-31 g(d)	0.40	–0.89	9.95	0.03	–1.25	9.59
M062x/6-311+G(d)//3-21G	–5.88	–6.84	3.38	–5.32	–6.29	3.93
TPSS/6-311+G(d)//3-21G	–4.45	–5.27	4.64	–4.72	–5.53	4.37
BMK/6-311+G(d)//3-21G	–3.56	–4.45	5.64	–2.10	–2.99	7.10
BHandHLYP/6-311+G(d)//3-21G	2.53	1.59	11.79	3.86	2.92	13.12
B2PLYPD/6-311+G(d)//3-21G	3.80	2.32	13.42	4.20	2.73	13.82

^a Including ZPE corrections.

TABLE 8: Energies^a (ΔE), Enthalpies (ΔH), and Gibbs (ΔG) Free Energies of the •OH Reactions with Pristine SCNTs, in kcal/mol, Computed at 298 K, Using Different Levels of Theory

	Gas		Benzene			
	ΔE	ΔH	ΔG	ΔE	ΔH	ΔG
B3LYP/6-311+G(d)//3-21G						
(3,3)	–42.74	–43.66	–33.42	–44.59	–41.49	–42.41
(5,0)	–53.73	–54.61	–44.31	–55.90	–52.39	–53.27
B3LYP/6-311+G(d)//6-31+G(d)						
(3,3)	–42.97	–43.95	–33.62	–45.01	–41.87	–42.85
(5,0)	–53.51	–54.42	–44.15	–55.89	–52.31	–53.23
M062x/6-311+G(d)//3-21G						
(3,3)	–46.58	–47.59	–37.17	–49.35	–46.08	–47.09
TPSS/6-311+G(d)//3-21G						
(3,3)	–45.91	–46.94	–36.45	–50.16	–46.61	–47.64

^a Including ZPE corrections.

2X, TPSS, and BMK functionals are lower (less positive). For this system, it should be noticed that, due to the magnitude of the ΔH values, that is, they are not as large as those for reactions involving SWCNTs, BHandHLYP and B2PLYPD functionals predict the reaction to be endothermic, whereas all the other tested functionals predict it as exothermic. For the modeled $\bullet\text{OH} + \text{SWCNTs}$ reactions, on the other hand, the ΔH and ΔG values are negative enough (more negative than 40 and 30 kcal/mol, respectively) and all the tested levels of theory predict the process as significantly exothermic and exergonic. In fact, the functional dependency was found to be smaller for the reactions involving SWCNTs than for those involving coronene.

In summary, the agreement among the predictions for the SWCNTs + $\bullet\text{OH}$ reactions obtained at all the tested levels of theory supports the reliability of the results presented in this work. Energy values for reactions of SWCNTs with free radicals are proposed to be more influenced by the functional of choice than by the size of the basis set.

Conclusions

The effect of carboxylation on the free radical scavenging activity of SWCNTs is predicted to depend on the functionalization site. If the carboxylation is at the open ends of the tubes, the free radical scavenging remains almost the same than that of the nonfunctionalized armchair fragments and decreases for the zigzag tubes. However, even for the zigzag fragments, the processes remain significantly exergonic, indicating that they are still expected to be great free radical scavengers. If the functionalization occurs at the tubes' walls, some sites of reaction become more reactive and some less reactive than those on the pristine SWCNTs. Assuming that the reactions take place at the most reactive sites, it can be concluded that the presence of $-\text{COOH}$ groups would increase the free radical scavenging activity of SWCNTs, provided that the coverage occurs in such an amount that there is enough free space on the walls for the reactions to take place. The predictions made in the present work at the B3LYP/6-311+G(d)//3-21G level of theory has been validated by comparison with other levels of theory.

Acknowledgment. This study was made possible due to funding from the Consejo Nacional de Ciencia y Tecnología (CONACyT) as well as resources provided by the Instituto de Investigaciones en Materiales IIM, UNAM. The work was carried out, using a KanBalam supercomputer, provided by DGSCA, UNAM, and the facilities at Laboratorio de Supercomputo y Visualización en Paralelo of UAM Iztapalapa. A.M. is grateful for financial support from DGAPA-UNAM-México.

Supporting Information Available: Energies of reaction, including zero-point energy corrections, and IR bands corresponding to the attached fragments. This material is available free of charge via the Internet at <http://pubs.acs.org>.

References and Notes

- (1) Tasis, D.; Tagmatarchis, N.; Bianco, A.; Prato, M. *Chem. Rev.* **2006**, *106*, 1105.
- (2) Dujardin, E.; Ebbesen, T. W.; Krishnan, A.; Treacy, M. M. *J. Adv. Mater.* **1998**, *10*, 1472.
- (3) Chen, Y.; Haddon, R. C.; Fang, S.; Rao, A. M.; Eklund, P. C.; Lee, W. H.; Dickey, E. C.; Grulke, E. A.; Pendergrass, J. C.; Chavan, A.; Haley, B. E.; Smalley, R. E. *J. Mater. Res.* **1998**, *13*, 2423.
- (4) Hiura, H.; Ebbesen, T. W.; Tanigaki, K. *Adv. Mater.* **1995**, *7*, 275.

- (5) Ebbesen, T. W.; Hiura, H.; Bisher, M. E.; Treacy, M. M. *J. Shreeve-Keyer, J. L.; Haushalter, R. C. Adv. Mater.* **1996**, *8*, 155.
- (6) Ebbesen, T. W. *Acc. Chem. Res.* **1998**, *31*, 558.
- (7) Dujardin, E.; Ebbesen, T. W.; Krishnan, A.; Tracey, M. M. *J. Adv. Mater.* **1998**, *10*, 611.
- (8) Rinzler, A. G.; Liu, J.; Dai, H.; Nikolaev, P.; Huffman, C. B.; Rodriguez-Macias, F. J.; Boul, P. J.; Lu, A. H.; Heymann, D.; Colbert, D. T.; Lee, R. S.; Fischer, J. E.; Rao, A. M.; Eklund, P. C.; Smalley, R. E. *Appl. Phys. A: Mater. Sci. Process.* **1998**, *67*, 29.
- (9) Kuznetsova, A.; Mawhinney, D. B.; Naumenko, V.; Yates, J. T.; Liu, J.; Smalley, R. E. *Chem. Phys. Lett.* **2000**, *321*, 292.
- (10) Ebbesen, T. W. *Acc. Chem. Res.* **1998**, *31*, 558.
- (11) Liu, J.; Rinzler, A. G.; Dai, H.; Hafner, J. H.; Bradley, R. K.; Boul, P. J.; Lu, A.; Iverson, T.; Shelimov, K.; Huffman, C. B.; Rodriguez-Macias, F.; Shon, Y.-S.; Lee, T. R.; Colbert, D. T.; Smalley, R. E. *Science* **1998**, *280*, 1253.
- (12) Mawhinney, D. B.; Naumenko, V.; Kuznetsova, A.; Yates, J. T. *J. Liu, J.; Smalley, R. E. Chem. Phys. Lett.* **2000**, *324*, 213.
- (13) Hu, H.; Bhowmik, P.; Zhao, B.; Hamon, M. A.; Itkis, M. E.; Haddon, R. C. *Chem. Phys. Lett.* **2001**, *345*, 25.
- (14) Sayes, C. M.; Liang, F.; Hudson, J. L.; Mendez, J.; Guo, W.; Beach, J. M.; Moore, V. C.; Doyle, C. D.; West, J. L.; Billups, W. E.; Ausmanb, K. D.; Colvin, V. L. *Toxicol. Lett.* **2006**, *161*, 135.
- (15) Watts, P. C. P.; Fearon, P. K.; Hsu, W. K.; Billingham, N. C.; Kroto, H. W.; Walton, D. R. M. *J. Mater. Chem.* **2003**, *13*, 491.
- (16) Fenoglio, I.; Tomatis, M.; Lison, D.; Muller, J.; Fonseca, A.; Nagy, J. B.; Fubini, B. *Free Radical Biol. Med.* **2006**, *40*, 1227.
- (17) Galano, A. *J. Phys. Chem. C* **2008**, *112*, 8922.
- (18) Lucente-Schultz, R. M.; Moore, V. C.; Leonard, A. D.; Price, B. K.; Kosynkin, D. V.; Lu, M.; Partha, R.; Conyers, J. L.; Tour, J. M. *J. Am. Chem. Soc.* **2008**, *131*, 3934.
- (19) Galano, A. *J. Phys. Chem. C* **2009**, *113*, 18487.
- (20) Galano, A. *Nanoscale* **2010**, *2*, 373.
- (21) Frisch, M. J.; Trucks, G. W.; Schlegel, H. B.; Scuseria, G. E.; Robb, M. A.; Cheeseman, J. R.; Montgomery, J. A., Jr.; Vreven, T.; Kudin, K. N.; Burant, J. C.; Millam, J. M.; Iyengar, S. S.; Tomasi, J.; Barone, V.; Mennucci, B.; Cossi, M.; Scalmani, G.; Rega, N.; Petersson, G. A.; Nakatsuji, H.; Hada, M.; Ehara, M.; Toyota, K.; Fukuda, R.; Hasegawa, J.; Ishida, M.; Nakajima, T.; Honda, Y.; Kitao, O.; Nakai, H.; Klene, M.; Li, X.; Knox, J. E.; Hratchian, H. P.; Cross, J. B.; Bakken, V.; Adamo, C.; Jaramillo, J.; Gomperts, R.; Stratmann, R. E.; Yazyev, O.; Austin, A. J.; Cammi, R.; Pomelli, C.; Ochterski, J. W.; Ayala, P. Y.; Morokuma, K.; Voth, G. A.; Salvador, P.; Dannenberg, J. J.; Zakrzewski, V. G.; Dapprich, S.; Daniels, A. D.; Strain, M. C.; Farkas, O.; Malick, D. K.; Rabuck, A. D.; Raghavachari, K.; Foresman, J. B.; Ortiz, J. V.; Cui, Q.; Aboul, A. G.; Clifford, S.; Cioslowski, J.; Stefanov, B. B.; Liu, G.; Liashenko, A.; Piskorz, P.; Komaromi, I.; Martin, R. L.; Fox, D. J.; Keith, T.; Al-Laham, M. A.; Peng, C. Y.; Nanayakkara, A.; Challacombe, M.; Gill, P. M. W.; Johnson, B.; Chen, W.; Wong, M. W.; Gonzalez, C.; Pople, J. A. *Gaussian 03*, revision D.01; Gaussian, Inc.: Wallingford, CT, 2004.
- (22) Cances, M. T.; Mennucci, B.; Tomasi, J. *J. Chem. Phys.* **1997**, *107*, 3032.
- (23) Mennucci, B.; Tomasi, J. *J. Chem. Phys.* **1997**, *106*, 5151.
- (24) Mennucci, B.; Cances, E.; Tomasi, J. *J. Phys. Chem. B* **1997**, *101*, 10506.
- (25) Tomasi, J.; Mennucci, B.; Cances, E. *THEOCHEM* **1999**, *464*, 211.
- (26) Okuno, Y. *Chem.—Eur. J.* **1997**, *3*, 210.
- (27) Benson, S. W. *The Foundations of Chemical Kinetics*; Krieger: Malabar, FL, 1982.
- (28) Ardura, D.; Lopez, R.; Sordo, T. L. *J. Phys. Chem. B* **2005**, *109*, 23618.
- (29) Alvarez-Idaboy, J. R.; Reyes, L.; Cruz, J. *Org. Lett.* **2006**, *8*, 1763.
- (30) Alvarez-Idaboy, J. R.; Reyes, L.; Mora-Diez, N. *Org. Biomol. Chem.* **2007**, *5*, 3682.
- (31) Galano, A. *J. Phys. Chem. A* **2007**, *111*, 1677.
- (32) Galano, A.; Cruz-Torres, A. *Org. Biomol. Chem.* **2008**, *6*, 732.
- (33) Galano, A.; Francisco-Márquez, M. *Chem. Phys.* **2008**, *345*, 87.
- (34) Mora-Diez, N.; Keller, S.; Alvarez-Idaboy, J. R. *Org. Biomol. Chem.* **2009**, *7*, 3682.
- (35) Naseh, M. V.; Khodadadi, A. A.; Mortazavi, Y.; Sahraei, O. A.; Pourfayaz, F.; Sedghi, S. M. *World Acad. Sci., Eng. Technol.* **2009**, *49*, 177.
- (36) Vossoughi, M.; Gojini, S.; Kazemi, A.; Alemzadeh, I.; Zeinalic, M. *Eng. Lett. [Online]* **2009**, *17*. Published Online: Nov 19, 2009.
- (37) Feng, J.; Sui, J.; Cai, W.; Gao, Z. *J. Compos. Mater.* **2008**, *42*, 1587.
- (38) Kim, W. J.; Kang, S. O.; Ah, C. S.; Lee, Y. W.; Ha, D. H.; Choi, I. S.; Yun, W. S. *Bull. Korean Chem. Soc.* **2004**, *25*, 1301.
- (39) Saini, R. K.; Chiang, I. W.; Peng, H.; Smalley, R. E.; Billups, W. E.; Hauge, R. H.; Margrave, J. L. *J. Am. Chem. Soc.* **2003**, *125*, 3617.
- (40) Galano, A. *J. Phys. Chem. A* **2007**, *111*, 1677.
- (41) Gauden, P. A.; Winiowski, M. *Catal. Today* **2010**, *150*, 147.

- (42) Adriaens, D. A.; Goumans, T. P. M.; Catlow, C. R. A.; Brown, W. A. *J. Phys. Chem. C* **2010**, *114*, 1892.
- (43) Zhao, Y.; Truhlar, D. G. *Theor. Chem. Acc.* **2008**, *120*, 215.
- (44) Tao, J.; Perdew, J. P.; Staroverov, V. N.; Scuseria, G. E. *Phys. Rev. Lett.* **2003**, *91*, 146401.
- (45) Boese, A. D.; Martin, J. M. L. *J. Chem. Phys.* **2004**, *121*, 3405.
- (46) As implemented in Gaussian 09: $0.5 * E_X^{HF} + 0.5 * E_X^{LSDA} + 0.5 * \Delta E_X^{Becke88} + E_C^{LYP}$.
- (47) Schwabe, T.; Grimme, S. *Phys. Chem. Chem. Phys.* **2007**, *9*, 3397.

(48) Grimme, S. *J. Chem. Phys.* **2006**, *124*, 034108.

(49) Alvarez-Idaboy, J. R.; Galano, A. Counterpoise corrected interaction energies are not systematically better than uncorrected ones: Comparison with CCSD(T) CBS extrapolated values. *Theor. Chem. Acc.* [Online early access]. DOI: 10.1007/s00214-009-0676-z. Published Online: Nov 13, **2009**.

JP100065T